Numerical calculations of the singular stress fields of failing mode-II cracks in comparison to experiments

A. Blázquez[1], J.F. Kalthoff[2], I. Palomino[3], A. Fernández-Canteli[4]

Summary

The stress fields at initiation of a kinked crack starting from a crack subjected to mode-II loading conditions is investigated. Special emphasis is given to the changes the stress fields experience in the transition phase from before to after the kinked crack is initiated. The stress field that builds up at the corner notch after the kinked crack initiated is also studied for comparison. The BEM, due to its inherent high spatial resolution, is used as an adequate technique for this kind of investigations. The validity of the numerical data is confirmed by experimental results obtained by caustic and photoelastic techniques.

Introduction

A crack subjected to shear (mode-II) conditions of loading (denoted mother crack) in brittle materials fails by initiating a tensile (mode-I) kinked crack (denoted daughter crack) propagating at an angle of about -70° with respect to the direction of the original mother crack. Between the mother crack and the daughter crack a notch is formed.

This paper is aimed to investigate the transition of the mode-II crack tip stress singularity of the mother crack before instability to the two singularities after instability, i.e. the mode-I singularity at the daughter crack and the additional stress singularity at the notch that is formed. In consideration of the very high resolution needed to accomplish this task, the BEM was considered, primarily due to the precision required for determining the stress fields in the immediate vicinity of the crack tip but also because of the short lengths considered for the daughter crack. The feasibility of the BEM-calculations for such fracture mechanics applications are confirmed by comparison with experimental results obtained using caustic and photoelastic techniques.

Numerical calculations

The boundary element calculations are performed for an Arcan-Richard-

[1] Dept. of Mechanical Engineering, University of La Rioja. C/ Luis de Ulloa, 20. 26004 Logroño, Spain
[2] Dept. of Experimental Mechanics, Ruhr-University Bochum. Universitätsstr. 150, 44780 Bochum, Germany
[3] School of Engineering. University of Sevilla. Camino de los Descubrimientos s/n. 41092 Sevilla, Spain
[4] Dept. of Const. and Manufacturing Engng. University of Oviedo. Campus de Viesques, 33203 Gijón, Spain

type specimen of width W = 50 mm prepared with a pre-existing crack of length of half the width, see Fig. 1a,b. The specimen size is chosen to be in accordance with practical test data that apply for measuring the fracture toughness of the aluminium alloy Al 7075 (E = 71000 MPa, ν = 0.34, $R_{p0.2}$ = 533 MPa, K_{Ic} = 30 MPa m$^{1/2}$, K_{IIc} = 44.4 MPa m$^{1/2}$).

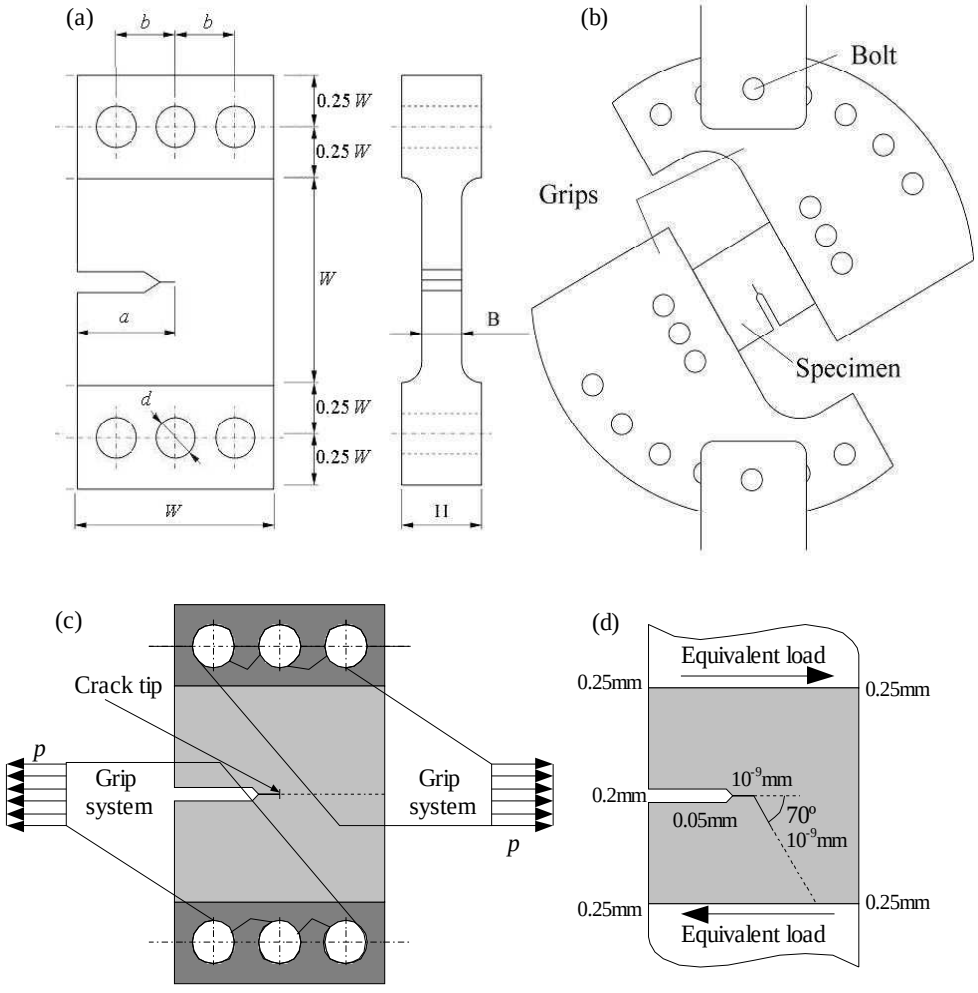

Fig. 1: Arcan-Richard set-up: a) specimen, b) grips, c) complete model used in the numerical calculation, d) simplified model and mesh size.

For the solution of the elastic problem, a plane model under plane strain conditions is considered using a multibody approach. Six bodies are considered initially as shown in Fig. 1c: Two solids represent the field of interest of the specimen where the cracks are located. Two other solids constitute the fixing zones

(dark grey); for these reinforced zones a Young modulus 10 times higher than that of the base material is used. For the last two solids representing the grips a stiffness 1000 times higher than that of the base material is assumed [1].

All the calculations were performed with the aid of a boundary element code, based on linear elements [2], assuming weak solutions for the boundary and interface conditions [3] with limitations of the rigid solid motion according to the formulation proposed by [4]. Figure 1d shows the approximate size of the elements in the significant regions of the boundary element model. The sizes have been maintained for all the calculations carried out.

Solving the foregoing problem allows one to establish the interactions among the different solids, particularly among the solids defining the thickened parts of the specimens and the ones concerning the field of study. Assuming these interactions not being changed during the process, the stress field in the vicinity of the crack can be analyzed for different crack lengths, see Fig. 1d. The interface among the solids is defined as having an inclination of −70°, with respect to the crack plane of the original mode-II mother crack.

Numerical and experimental results

The stress field results are shown in the form of angular distributions at various distances from the singularity origin and in the form of contour lines of principal stress differences.

Angular stress distributions at various radial distances:

The results are presented with respect to three coordinate systems with origins at the tip of the corresponding stress singularities (see Fig. 2). The indices *M*, *D*, and *N* are used for characterizing the mother crack, the daughter crack, and the notch , respectively. The stress field singularities at the tip of the mother crack and

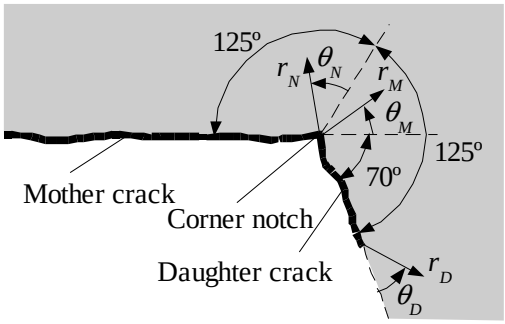

Fig. 2: Coordinate systems considered in the present study for the original mother crack, for the kinked daughter crack and for the corner notch, built between the two.

the daughter crack are found to show a $r^{-0.5}$ dependence (as expected in fracture mechanics). The singularity coefficient of the notch, howerver, results to 0.41 in accordance with the results in [5] for a notch of an opening angle of 250°. In Fig. 3 the stresses, multiplied by the singularity dependence, are plotted for a length of the daughter crack of 0.1 mm. In all cases the results are normalized by the stress

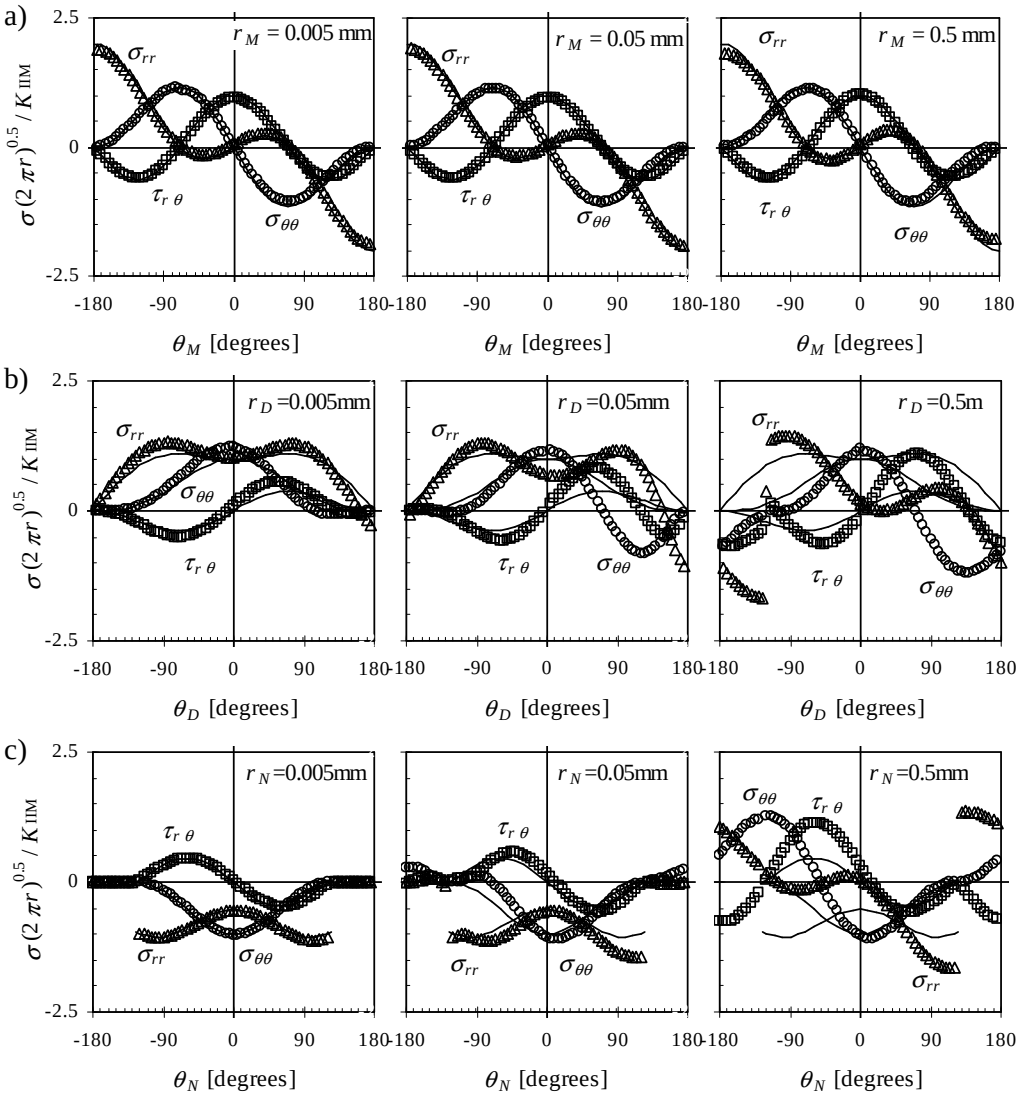

Fig. 3: Angular stress distributions at varying distances, r, from singularity as a function of the respective angular orientations θ_M, θ_D and θ_N: a) around the tip of the mother crack, b) around the tip of the daughter crack and c) around the corner notch.

intensity factor of the mother crack K_{IIM}. The stresses around the singularity are given at different radial distances r. The corresponding analytical results of the near tip stress fields for mode-II or for mode-I loading [6] are also given (continuous line) for comparison.

Figure 3a shows the numerical results for the original mother crack before the daughter crack arises ($a_D = 0$, reference angle θ_M). For circles of different radii the numerical results are practically coincident with the analytical ones for a typical mode-II stress field. Figure 3b shows the normalized stress distributions around the tip of the daughter crack. The stress field for a very small value of r (compared to the crack length) approaches notably a typical mode-I stress field. For distances far away from the crack tip (compared to the crack length), a mode-II stress field, i.e. the stress field of the mother crack, results. Please note, the angle θ_D is shifted in relation to θ_M (used in Fig. 3a) due to the different reference axes used. Figure 3c gives the singular stress field that was found around the corner notch. This stress field for small radial distances agrees well with the results for the stress distribution around a notch (250° opening angle) derived analytically in [5]. It is recognized that the stress field is of compressive character. At large distances (compared to the length of the daughter crack), when the corner notch is circumscribed, the mode-II stress field around the mother crack results (see Fig. 3a for comparison: again note the shift due to the differently defined angles used).

Similar results as reported were found for shorter and larger lengths of the

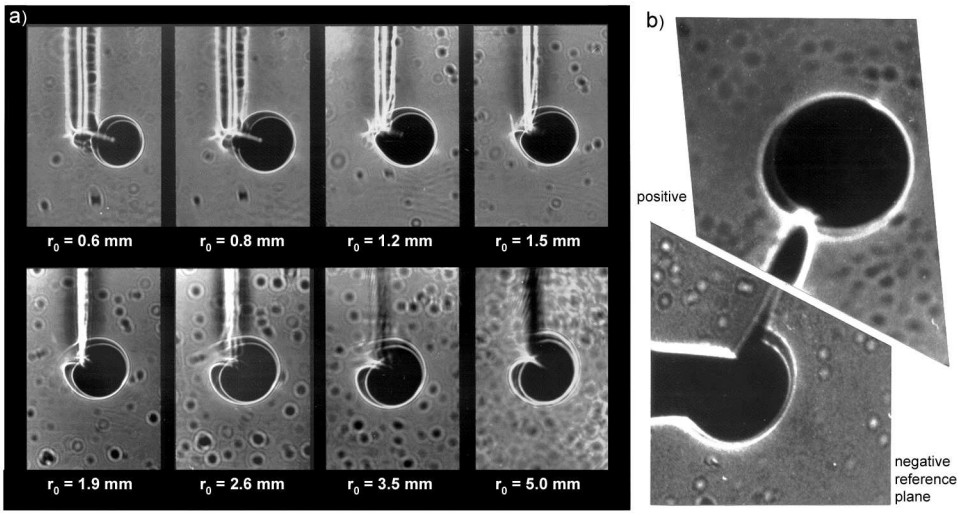

Fig. 4: Shadow optical caustic images for the configuration: mother crack, daughter crack and corner notch, a) for various radii of the shadow optical initial curves and b) for positive (upper) and negative (lower) reference.

daughter crack ($a_D = 0.01$ and 1 mm, or even longer lengths) not given here because of space limitations, see [7].

Shadow optical caustic investigations were performed [8, 9] and are used for comparing the numerical with experimental results. Based on the stresses at a circular contour around the stress singularity of given radius r_o, i.e. the so-called initial curve, caustics of different geometrical shape and size are generated depending on the character of the stress field [10]. For a given stress singularity, the radius r_o of the initial curve is controlled by optical parameters of the measuring arrangement and can, thus, be varied.

Figure 4a shows shadow optical caustic images for the configuration of a mode-II loaded mother crack of 50 mm length and a 2 mm long daughter crack at an angle of 70° in a specimen made of the epoxy resin Araldite B. For small initial radii r_o (0.6 mm) the observed caustic is a typical mode-I caustic (see also Fig. 4b, upper part); for larger initial radii (5 mm) the caustic is a typical mode-I caustic representing the loading condition of the original mother crack. At the corner notch a light concentration area is observed in Fig. 4a, for better visualization shown in Fig. 4b as a dark shadow spot in a reference plain of negative sign, indicating a compressive stress concentration at the corner notch [9, 10] (please note the different orientations of crack configuration and loading). These experimental observations are in full agreement with the BEM results of Fig. 3.

Contour lines of principal stress differences:

The numerical BEM results are further used to calculate contour lines of principle stress differences which are experimentally observed as so-called

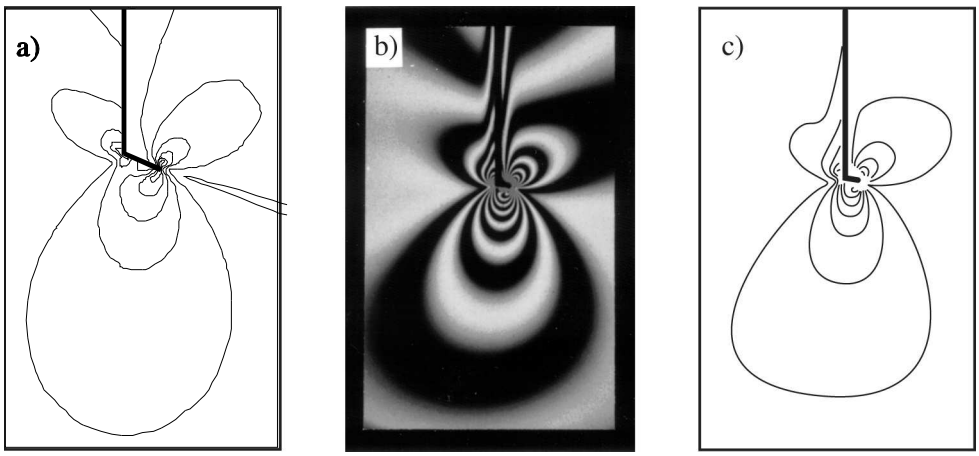

Fig. 5: Isochromatic fringes for configuration: mother crack, daughter crack and corner notch, a) BEM calculation, b) photoelastic recording and c) selected discrete lines of b).

isochromatic fringes by photoelastic techniques. These fringes assume characteristic geometrical shapes and sizes for particular stress concentration fields. Figure 5a shows the numerically calculated fringes; Figures 5b and 5c give the experimentally observed fringes for experimental conditions as reported above [8, 9]. In close neighbourhood of the stress origins the mode-I singular stress field at the tip of the daughter crack and the symmetric compressive stress field at the corner notch, as well as the mode-II stress field formed at larger distances are clearly identified and in good agreement with the BEM results.

Conclusions

The BEM is found a suitable method to perform numerical calculations for complex problems in fracture mechanics as those related to mode-II or mixed mode loaded cracks for which failure is associated with both a change in the type of the stress singularity and an increase in the number of the stress singularities involved. This is demonstrated for the transition of a shear mode-II singularity of a mother crack into the mode-I singularity around the daughter crack tip and a compression singularity around the corner notch. Both stress fields are of symmetric nature although loading and crack geometry are not symmetric.

The calculations have shown that the mode-I stress field around the tip of the daughter crack builds up as a consequence of the existence of the daughter crack, in particular also for very small length of the daughter crack. It must be recognized, though, that the K_I dominated region is arbitrarily small. The BEM results are compared to and were found to be in good agreement with results of experimental investigations by shadow optical and photoelastic techniques.

The high spatial resolution of the BEM was the essential prerequisite for performing the study as reported.

References

1 Morales, P., Blázquez, A., Fernández, D. and Kalthoff, J.F. (2003): "Investigation of the suitability of a test method for determining mode-II fracture toughnesses using boundary element analysis", Advances in Boundary Element Techniques IV, Gallego and Aliabadi Eds. (2003).

2 París, F. and Cañas J. (1997): *Boundary Element Method*, Oxford Univ. Press.

3 Blázquez, A., Mantič, V., París, F. and Cañas, J (1996): "On the removal of rigid body motions in the solution of elastostatic problems by direct BEM", *Int. J. for Numerical Methods in Engng.*, 39, 23, pp. 4021-4038 (1996).

4 Blázquez, A., Mantič, V., París, F. and Cañas J. (1998): "BEM solutions of contact problems by weak application of contact conditions with non-conforming discretizations", *Int. J. of Solids and Structures*, 35, 24, pp. 3259-3278.

5 Williams, W.L. (1952) "Stress singularities resulting from various boundary conditions in angular corners of plates in extension", *Journal of Applied Mechanics*, Trans. ASME, Dec., pp. 526-528.

6 Kanninen, M.F.and Popelar, C.H. (1985): *Advanced Fracture Mechanics*, Oxford Univ. Press.

7 Blázquez, A., Kalthoff, J.F., Palomino, I. and Fernández-Canteli, A. (2204): "Application of the BEM for determining singular stress fields for the conditions of failing mode-II cracks", BeTeQ2004, Lissabon.

8 Podleschny, R. (1995): *Untersuchungen zum Instabilitätsverhalten scher-beanspruchten Risse*. Doctoral Thesis. Institut für Mechanik, Ruhr-Universität Bochum.

9 Kalthoff, J.F. (2000) "Modes of dynamic shear failure in solids", *Int.Journal of Fatigue*, 101, pp. 1-31.

10 Kalthoff, J.F. (1993) "Shadow optical method of caustics" Chapter 9 in *Handbook on Experimental Mechanics* (Edited by A.S. Kobayashi). 2nd revised edition, VCH Publishers, New York, pp. 407-476.